CrossMark
click for updates

Precise control over reduction potential of fulleropyrrolidines for organic photovoltaic materials†

M. Karakawa,*[ab] T. Nagai,[c] K. Adachi,[c] Y. Ie[b] and Y. Aso*[b]

Organic photovoltaic cells based on two types of organic materials (acceptor and donor) have attracted considerable attention for their low-cost fabrication, and potential for realization of flexible and light weight devices. For many years organic photovoltaic cells have relied on [6,6]-phenyl C_{61} butyric acid methyl ester, a fullerene derivative that is used as an electron acceptor material. A few reports on bisadduct and C_{70} derivatives have shown some improvements in device performance; however, further enhancements based on improvements to the fullerene acceptor component have proven challenging. Here we described the device performance of improved acceptor fullerene materials that allow the open circuit voltage to be fine-tuned in organic photovoltaic cells to provide high power conversion efficiency. Our new approach to designing fullerene materials will accelerate development of n-type semiconductor materials and allow for new low cost organic photovoltaic cells.

Introduction

Environmentally friendly energy generation is an important global issue for society. Solar energy harvesting has been recognized as an effective way of addressing our increasing energy needs. Organic photovoltaic (OPV) cells have attracted great attention in recent years owing to the simplicity of their fabrication processes, such as low-cost printing techniques.[1–5]

Current state-of-the art OPV cells are fabricated as a thin film comprising a mixture of p- and n-type organic semiconducting materials.[1,2] This organic semiconducting film features a nano-scale phase-segregated structure known as a bulk-hetero junction (BHJ), which provides an effective pathway for a charge generation and separation in the film.

The p-type semiconductors used in such devices are π-conjugated aromatic compounds based on polymers and small molecules, which absorb light leading to generation of excitons in the film.[1,2] The absorption of the p-type materials is related to their chemical structures and directly affects their performance

in devices. Over the past decade many types of p-type materials have been developed and OPV cells with power conversion efficiencies greater than 10 or 11% have been reported.[6–10]

In contrast to the remarkable development of p-type donor materials, for n-type acceptor materials there have been few advances over [6,6]-phenyl C_{61} butyric acid methyl ester ($PC_{61}BM$), which has dominated reports in this field over the last decade.[11] In the term, indene bis-adduct C_{60} derivative ($IC_{60}BA$), which is one of the important fullerene derivative, presented an effect to changing a LUMO energy level contributing to obtain a high voltage in OPV cells.[12] While a few other n-type materials based on fullerenes have been reported,[13–23] the development of non-fullerene acceptors and n-type semiconductors for use in OPV cells has become an active area of research.[24–31] Although interest has shifted to non-fullerene derivatives, it remains important to develop new fullerenes as low-cost acceptor materials that may allow for commercially viable OPV modules.

We have previously reported the synthesis and application of new fulleropyrrolidine derivatives having various substituents.[32] Our previous study indicated that *N*-phenyl fulleropyrrolidine and its OPV cells showed a higher reduction potential and better device performance, respectively, than those based on $PC_{61}BM$.

In this paper, we show that the reduction potential of fulleropyrrolidine derivatives can be controlled based on the structure of the substituent groups. These modifications can in turn control and enhance the open circuit voltage (V_{oc}) of OPV cells. Our newly synthesized fulleropyrrolidine derivatives were designed based on theoretical calculations. The synthesized materials were characterized by UV-vis absorption, cyclic

[a]Institute for Frontier Science Initiative, Kanazawa University, Kakuma-machi, Kanazawa, Ishikawa 920-1192, Japan. E-mail: karakawa@staff.kanazawa-u.ac.jp; Fax: +81-76-234-4780

[b]Department of Soft Nanomaterials, Nanoscience and Nanotechnology Center, The Institute of Scientific and Industrial Research (ISIR), Osaka University, 8-1 Mihogaoka, Osaka 567-0047, Ibaraki, Japan. E-mail: aso@sanken.osaka-u.ac.jp; Fax: +81-6-6879-8479

[c]Fundamental Technology Group, Chemical R&D Center, Daikin Industries, Ltd, 1-1 Nishi Hitotsuya, Osaka 566-8585, Settsu, Japan. Fax: +81-6-6349-4751

† Electronic supplementary information (ESI) available: Experimental information for synthesis of compounds, CV curves, atomic force microscopy images. See DOI: 10.1039/c6ra27661j

voltammetry and OPV cell measurements. Relationships between the substitution pattern and V_{oc} value were analysed in detail. An OPV cell based our C_{60}-fulleropyrrolidine derivative showed high power conversion efficiency (PCE) of 7.30% with a V_{oc} of 0.80 V. This fulleropyrrolidine represents a next generation fullerene acceptor, which may advance OPV performance beyond that which is possible with $PC_{61}BM$.

Results and discussion

Our new C_{60}-fulleropyrrolidine derivatives are illustrated in Fig. 1. Density functional theory (DFT) calculations of the fulleropyrrolidines were conducted, with Gaussian 09 at the B3LYP/6-31G level, to guide the design of novel fulleropyrrolidine derivatives before their synthesis as shown in Fig. 2 and 3. To simplify the calculations and ensure no-conjugation between the substituent group and the fullerene π-system, the calculations were performed about the substituent group and its surrounding structure.

The results of the calculated highest occupied molecular orbitals (HOMO) and lowest unoccupied molecular orbitals (LUMO) were related to the structures of the derivatives. When a fluorine (F) atom was introduced at the *ortho* position of the N-phenyl group (compounds **1** and **2**), the HOMO energy level was unchanged; however, compound **2** has a higher LUMO level than that of **1**. When an F atom was introduced at the *ortho* position of the C2 phenyl group (compounds **3** and **4**), the energy level changed in a similar way to that for compounds **1** and **2**; however, the effects were more pronounced in compounds **3** and **4**, which had lower LUMO energy levels. These calculations indicate that the energy levels were mainly affected by the number and position of the F atoms that were introduced into the N- and C2-phenyl groups.

When a methoxy group was introduced at the C2-phenyl group instead of an F atom, the energy levels of **5**, **6** and **7** shifted higher, as observed for the introduction of an F atom into the N-phenyl group (Fig. 3). In compound **7**, the combined effects of both the F atoms and the methoxy groups gave the
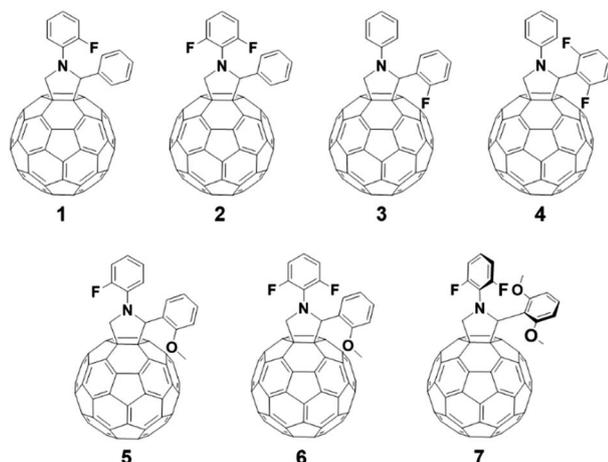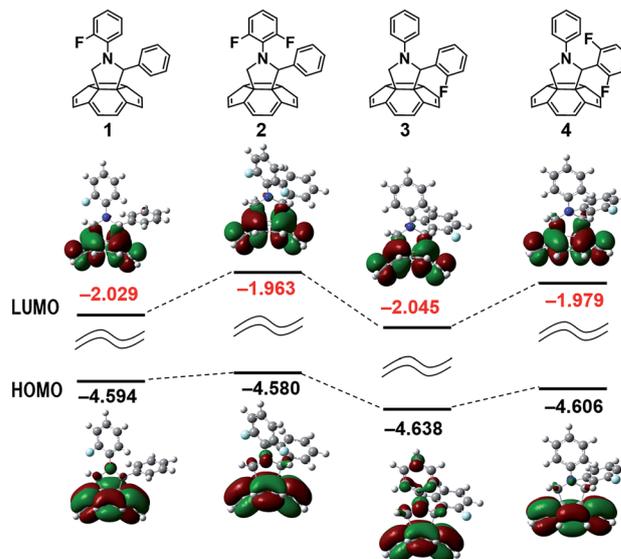

Fig. 2 DFT calculations for substituent groups and their surrounding structure (**1–4**).
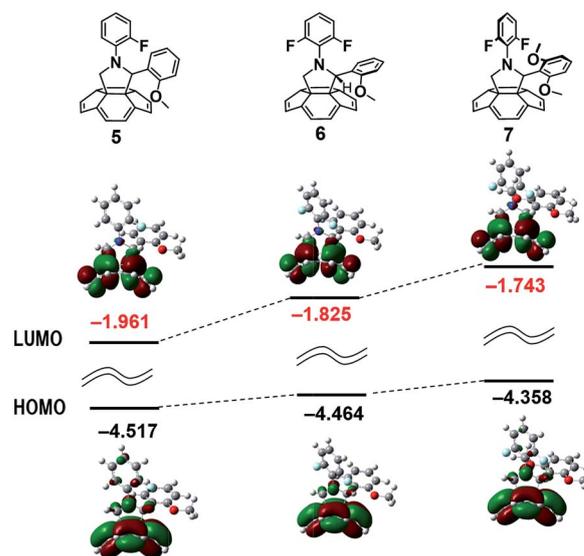

Fig. 3 DFT calculations for substituent groups and their surrounding structure (**5–7**).

highest calculated LUMO energy level in this series. Based on the LUMO level of our unsubstituted compound (PNP),[32] we could estimate a V_{oc} value of 0.82 V for **7** and 0.80 V for the mono-methoxy compound **6**. Notably these small changes in substitution might have a considerable influence on the LUMO level of the fulleropyrrolidine derivative but did not result in any break down of the fullerene π-system. Maintaining the fullerene π-system is important for forming an ideal BHJ structured thin film and for obtaining material that is stable under electron injection conditions.

We synthesized compounds shown in Fig. 1, **1–7** from corresponding amino acids and aldehyde derivatives under one
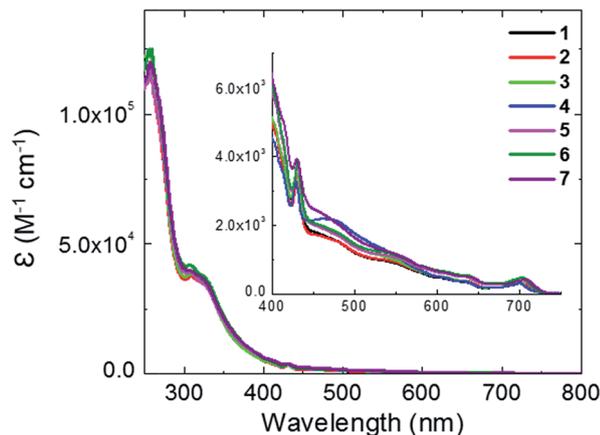

Fig. 1 C_{60}-Fulleropyrrolidine derivatives.

Fig. 4   UV-vis absorption spectra of fulleropyrrolidine derivatives.

step Prato reaction conditions.[33,34] The full synthetic procedures are described in ESI (Fig. S1†).

UV-vis absorption spectra for fullerene derivatives, **1–7**, were measured in chloroform solution (Fig. 4). An absorption band between 250 and 400 nm with a maximum located at 257 nm was observed in all compounds. A sharp peak at 420 nm, which is also observed for PC$_{61}$BM, was assigned to the 58π-system of the fullerene derivative. A weak absorption at 710 nm was attributed to π–π* transitions of the fullerenes. Small absorption differences were observed in the region between 430 and 600 nm, indicating that the substituent groups on the fullerenes

had little effect on the electronic structure of the fullerene π-system.

Cyclic voltammetry (CV) measurements were performed in a three-electrode cell to estimate the LUMO energy level of the derivatives from their reduction potential. The results obtained are summarized in Table 1. For comparison, the CV value of PNP[32] is also listed. Reversible redox processes were observed in all the fulleropyrrolidine derivatives, as shown in Fig. S2†. The following equation was used to calculate the LUMO levels: $E_{\text{LUMO}} = -(E^1_{1/2} + 4.8 \text{ eV})$, where $E^1_{1/2}$ is the first half-wave reduction potential relative to ferrocene (Fc).[35]

The reduction potentials of the fulleropyrrolidines varied depending on their substitution pattern as shown in Table 1. The LUMO energy level was raised by around 0.02 eV per F atom from **1** to **2**. The F atoms on the C2-phenyl group had little effect on the LUMO level and raised the energy by less than 0.01 eV per F atom. The trends of the CV results were consistent with the trends of our DFT calculations, as shown in Fig. 2. The DFT calculations indicated that the methoxy-substituted compound **7** would have the highest LUMO energy level, and indeed, **7** featured the most negative reduction potential in the series, as determined by CV. Notably there were no π-orbital interactions between the substituent group and the fullerene π-system. The differences in the reduction potentials were likely caused by through space π–π orbital interactions between the fullerene and the C2-phenyl ring. In a recent report, Swager and co-workers described a relationship between the cyclobutadiene structure and the fullerene π-system, which resulted in a higher LUMO level.[36]

Our CV results, suggest that the reduction potential can be controlled by introducing substituents that have through space interactions, but do not disrupt the fullerene π-system.

OPV cells were fabricated from the newly synthesized fulleropyrrolidine derivatives as acceptor materials and PTB7 as a donor material to evaluate the potential of the materials. A device structure of ITO/PFN/PTB7:fullerene derivative/MoO$_x$/Al under simulated AM 1.5G solar irradiation at 100 mW cm^{-2} was used. The active layer was spin-cast from chlorobenzene (CB) solutions for compounds **1**, **2**, **5** and **6**, and *o*-dichlorobenzene (DCB) solutions for **3**, **4** and **7** owing to the compounds different

Table 1   UV-vis and CV data for fullerene derivatives

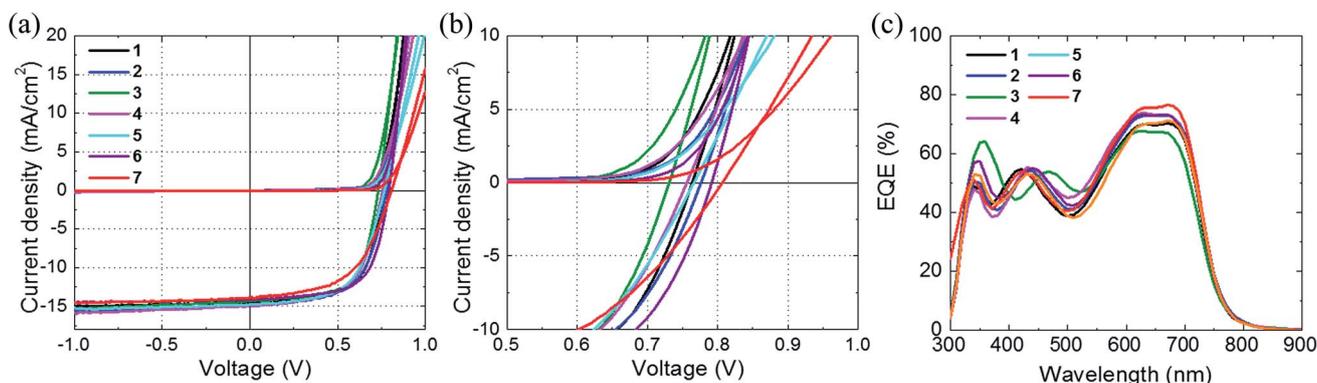| Compound	λ (nm)	ε (×10^5)	$E^1_{1/2}$ (V vs. Fc/Fc$^+$)	E_{LUMO} (eV)
1	255	1.18	−1.141	−3.659
2	256	1.15	−1.162	−3.638
3	256	1.23	−1.129	−3.671
4	256	1.19	−1.133	−3.667
5	257	1.20	−1.151	−3.651
6	257	1.25	−1.158	−3.642
7	257	1.20	−1.175	−3.625
PNP	257	1.12	−1.128	−3.672

Fig. 5   J−V curves for the ranges (a) −1.0 to 1.0 V and (b) 0.5–1.0 V, and (c) external quantum efficiency (EQE) spectra of OPV cells with fulleropyrrolidine derivatives.

Table 2 OPV performance of fulleropyrrolidine derivatives, 1–7[a]

	PTB7:1	PTB7:2	PTB7:3	PTB7:4	PTB7:5	PTB7:6	PTB7:7
J_{sc} [mA cm^{-2}]	14.468 (14.312 ± 0.305)	14.866 (14.507 ± 0.579)	14.327 (14.143 ± 0.376)	14.848 (13.997 ± 0.489)	14.758 (14.493 ± 0.325)	14.104 (14.105 ± 0.173)	13.875 (13.552 ± 0.235)
V_{oc} [V]	0.764 (0.761 ± 0.003)	0.776 (0.784 ± 0.005)	0.731 (0.734 ± 0.006)	0.756 (0.757 ± 0.005)	0.766 (0.768 ± 0.003)	0.792 (0.795 ± 0.003)	0.807 (0.809 ± 0.008)
FF	0.644 (0.631 ± 0.021)	0.614 (0.606 ± 0.019)	0.653 (0.631 ± 0.014)	0.613 (0.625 ± 0.007)	0.598 (0.593 ± 0.017)	0.654 (0.629 ± 0.036)	0.545 (0.538 ± 0.005)
PCE [%]	7.12 (6.87 ± 0.17)	7.09 (6.88 ± 0.17)	6.84 (6.54 ± 0.22)	6.88 (6.62 ± 0.19)	6.76 (6.59 ± 0.13)	7.30 (7.05 ± 0.33)	6.10 (5.90 ± 0.12)

[a] Mean values and standard deviations of 10 devices shown in parentheses.

solubilities. The current density–voltage (J–V) characteristics and the external quantum efficiency (EQE) spectra are shown in Fig. 5. The OPV parameters are summarized in Table 2. As reported by Janssen and co-workers $PC_{71}BM$-based OPV devices generally show higher performance than those based on $PC_{61}BM$, which has been attributed to the broader absorption of $PC_{71}BM$ than that of $PC_{61}BM$.[37] However, C_{70} fullerene derivatives are expensive, which makes them less well suited to commercial production of OPV modules. We believe that development of C_{60} fullerene-based acceptors is important to realizing economically viable OPV cells. The data reported in Table 2 are comparable to reports on the performance of OPV cells with $PC_{71}BM$ as an acceptor.[38,39]

The J–V curves show that the devices generated high short circuit current density (J_{sc}) values. High J_{sc} values were achieved in OPV cells based on compounds 2 and 5. The device featuring compound 7 had a slightly lower J_{sc}, which was attributed to a thinner active layer (~90 nm) in this device and reduced photo absorption. The OPV cell with 7 also had a slightly higher series resistance than the others and a relatively low fill factor.

We focused on the V_{oc} of the OPV cells based on our new acceptors. Our CV measurements and calculations revealed a trend in the reduction potential of the compounds. The data in Table 2 and Fig. 5b clearly show that the V_{oc} values reflected the different reduction potentials of the derivatives. Relationships between the chemical structure and V_{oc} are illustrated in Fig. 6.

In changing the basic PNP structure (0.742 V, −3.672 eV), by introducing fluorine atoms in compounds 1 and 2, we observed that the V_{oc} increased by 0.02 eV per F atom and enhanced the V_{oc} to 0.78 V. For the case of C2-phenyl substitution the measured V_{oc} values were slightly lower than those of 1 and 2, even in compound 4, which had two F atoms. The C2-phenyl fluorination had little positive effect on the V_{oc} value. A tetra-fluoro compound (4F in ESI†) was also synthesized. The 4F showed above trade off relations of introducing F atoms in phenyl rings, resulting in not so high V_{oc} of 0.780 V.

For the methoxy-substituted series, V_{oc} increased to *ca.* 0.77, 0.80 and 0.81 for the OPV cells based on 5, 6 and 7, respectively.
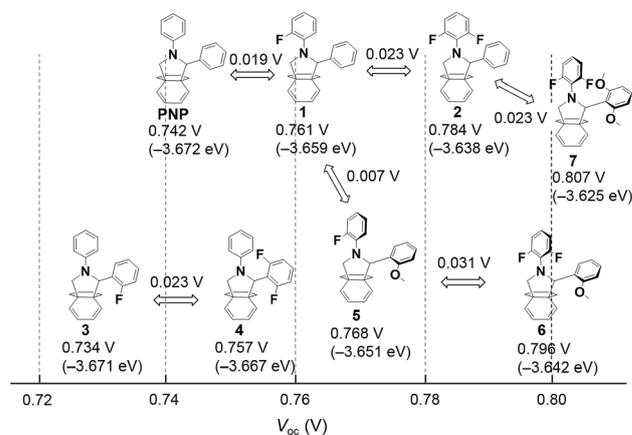

Fig. 6 Relationships between chemical structure and obtained V_{oc}. The values in brackets are the LUMO levels calculated from CV measurements.

This trend also agreed with the DFT calculations and CV results. Thus, the V_{oc} in cells with PTB7 (typically 0.74 V) was increased to more than 0.80 V without any disruption to the pristine fullerene π-system. We showed that modifying the substitution pattern is a promising method to fine tune the LUMO level of fullerene derivatives and achieve the best alignment of energy levels in a cell.

Conclusions

In conclusion, we designed new fulleropyrrolidine acceptor molecules guided by theoretical calculations. On the basis of these calculations we synthesized new fulleropyrrolidine derivatives with controlled reduction potentials. The trend in the LUMO levels of the compounds was determined by DFT calculations and was consistent with the results of CV measurements. We fabricated OPV devices and evaluated the performance of the compounds. Introduction of an F atom into the N-phenyl group contributed to enhanced V_{oc} of OPV cells. Conversely, an F atom on the C2 phenyl group made little contribution to the V_{oc} of OPV cells. The position and number of the F atoms introduced into the phenyl group affected the shifting of the LUMO level. Furthermore, compounds having methoxy-substituted C2 phenyl groups were used as acceptors in the active layer of OPV cells. The energy level of these derivatives also affected the V_{oc} value of the OPV cells. A V_{oc} as high as 0.81 V was achieved with PTB7 as the donor material. In this fulleropyrrolidine series, we were able to tune the V_{oc} value by 0.01–0.07 V without breaking the C_{60} fullerene π-system. We achieved a high PCE of 7.30% using our C_{60} fulleropyrrolidine derivatives. To date, development of new p-type materials with improved light absorption, have mainly contributed to improved energy conversion efficiency in OPV. In this report, we successfully improved the PCE of OPV cells with fulleropyrrolidine acceptor materials, by enhancing the V_{oc} of the cell. This is an important step that may contribute to new gains in already highly optimized OPV cells.

Experimental

Materials and methods

Materials. Reagents were purchased from Wako Pure Chemical Industries, Tokyo Kasei Chemical Industries, Merck, and Aldrich, and used without further purification. C_{60} fullerene was purchased from Honjo Chemical Corporation. PTB7 as a donor material for the OPV cells was purchased from 1-Material Chemscitech and was used as received. PFN[40] was synthesized in accordance with literature procedures. N-(2-Fluorophenyl)glycine and N-(2,6-difluorophenyl)glycine ethyl ester were prepared according to reported methods.[41,42]

General measurement and characterization. UV-visible spectra were recorded on a Shimadzu UV-3100PC. All spectra were obtained in spectroscopic grade solvents with quartz cells with a 1 cm path length. ^1H and ^{13}C NMR spectra were recorded with a Bruker Avance III (700 MHz) spectrometer in chloroform-d [chemical shifts in parts per million (ppm) downfield from tetramethylsilane as an internal standard for ^1H and ^{13}C]. ^{19}F

NMR was recorded with a JEOL JNM-ECS400 (400 MHz) spectrometer in chloroform-d [chemical shifts in parts per million (ppm) up field from fluorotrichloromethane as an internal standard for ^{19}F]. Cyclic voltammetry was performed on a BAS CV-50W voltammetric analyzer with Pt working and counter electrodes in chlorobenzene/CH_3CN (5/1, v/v) solution containing 0.1 mol L^{-1} Bu_4NPF_6. Column chromatography was performed with silica gel, (Kanto Chemical, silica-gel 60N, 40–50 μm). The fulleropyrrolidine compounds were further purified by recycling gel-permeation liquid chromatography (GPC) with a Japan Analytical Industry LC-908 equipped with JAI-GEL 1H/2H columns (eluent: $CHCl_3$) and with Cosmsil Bucky-prep® Columns (eluent: toluene). Elemental analyses were performed on a Perkin Elmer LS-50B by the Elemental Analysis Section of Comprehensive Analysis Center (CAC), ISIR, Osaka University. Surface morphologies of the deposited organic films were observed with an atomic force microscope (Shimadzu, SPM9600). The thicknesses of deposited organic films were measured with a KLA-Tencor alpha-step IQ surface measurement profiler.

OPV device fabrication and measurements. All cells were fabricated on 150 nm thick ITO-coated glass substrates that were detergent and solvent cleaned. For the inverted device structure, ITO/PFN/polymer : acceptor (1 : 1.5)/MoO_x/Al, the PFN interlayer material was dissolved in methanol (2 mg mL^{-1}) and spin-coated on top of the clean ITO substrate based on previous reports.[9] The organic active layer, with a thickness of 90–100 nm, was prepared by spin-coating a blended solution (25 mg mL^{-1}) in chlorobenzene (for **1**, **2**, **5** and **6**) with 1,8-diiodoctane (3%, v/v) or dichlorobenzene (for **3**, **4** and **7**) with 1,8-diiodoctane (3%, v/v) at 1000 rpm for 120 s in a nitrogen atmosphere. A 10 nm MoO_x layer and an 80 nm Al layer were then evaporated through a shadow mask to define the active area (0.09 cm^2) of the devices and form the top electrode using EO-5 metal evaporation chamber (Eiko engineering co. Ltd.). Current density–voltage characteristics of the photovoltaic cells were measured in the dark and under simulated solar light, with a Keithley 2400 source meter and a XES-301S solar simulator (San-Ei Electric Co., Ltd.), calibrated to produce 100 mW cm^{-2} AM 1.5G illumination. All device measurements were performed in N_2 filled measurement-apparatus at room temperature.

Synthesis

C_{60}-Fused N-(2-fluorophenyl)-2-phenylpyrrolidine (1). A chlorobenzene solution (100 mL) of the benzaldehyde (106 mg, 1 mmol), N-(2-fluorophenyl)glycine (169 mg, 1 mmol) and [60] fullerene (360 mg, 0.5 mmol) was stirred at 130 °C for 72 h and concentrated under reduced pressure. The product was separated by column chromatography (SiO$_2$, n-hexane : toluene, 20 : 1–5 : 1) and by GPC to give the compound **1** (177 mg, 38%); ^1H NMR (700 MHz, CDCl$_3$, δ): 4.74 (1H, d, J = 9.6 Hz), 5.66 (1H, d, J = 9.6 Hz), 6.10 (1H, s), 7.10–7.38 (7H, m), 7.77 (2H, d, J = 7.3 Hz); ^{19}F-NMR (372.5 MHz, CDCl$_3$, δ): −119.50 to −119.75 (m); ^{13}C NMR (175 MHz, CDCl$_3$, δ): 66.68, 66.71, 68.66, 75.91, 116.42 (d, $^2J_{FC}$ = 20.2 Hz), 123.77, 124.36 (d, $^3J_{FC}$ = 7.7 Hz), 128.37,

128.71, 128.82, 134.59 (d, $^2J_{FC}$ = 10.6 Hz), 135.86, 136.06, 136.59, 136.65, 136.88, 139.34, 139.83, 140.22, 140.26, 141.49, 141.68, 141.88, 141.93, 142.02, 142.05, 142.08, 142.14, 142.20, 142.23, 142.41, 142.59, 142.61, 142.72, 143.00, 143.18, 144.38, 144.43, 144.60, 144.78, 145.19, 145.28, 145.29, 146.34, 145.44, 145.46, 145.55, 145.63, 145.79, 145.97, 146.04, 146.15, 146.18, 146.25, 146.28, 146.33, 146.36, 146.46, 146.87, 147.36, 147.40, 152.99, 153.49, 156.02, 157.81 (d, $^1J_{FC}$ = 248.5 Hz); UV-vis (CHCl$_3$): λ_{max} (ε) = 255 nm (118 000); MS (FAB) m/z 934 (M + 1); HRMS calcd for C$_{74}$H$_{13}$FN 934.1032; found 934.1052; calcd C 95.17, H 1.30, N 1.50; found C 95.25, H 1.78, N 1.55.

C$_{60}$-Fused N-(2,6-difluorophenyl)-2-phenylpyrrolidine (2). A chlorobenzene solution (100 mL) of the benzaldehyde (212 mg, 2 mmol), N-(2,6-difluorophenyl)glycine (187 mg, 1 mmol) and [60]fullerene (360 mg, 0.5 mmol) was stirred at 130 °C for 96 h and concentrated under reduced pressure. The product was separated by column chromatography (SiO$_2$, n-hexane : toluene, 20 : 1–5 : 1) and by GPC to give the compound 2 (108 mg, 23%); ^{1}H NMR (700 MHz, CDCl$_3$, δ): 5.12 (1H, d, J = 9.1 Hz), 5.26 (1H, d, J = 9.1 Hz), 6.46 (1H, s), 6.96 (2H, t, J = 8.7 Hz), 7.12–7.35 (4H, m), 7.77 (2H, d, J = 7.5 Hz); ^{19}F-NMR (372.5 MHz, CDCl$_3$, δ): −117.06 to −117.15 (m); ^{13}C NMR (175 MHz, CDCl$_3$, δ): 65.73, 68.93, 76.51, 77.84, 112.42 (d, $^2J_{FC}$ = 20.4 Hz), 122.15 (t, $^2J_{FC}$ = 13.9 Hz), 126.89 (t, $^3J_{FC}$ = 10.2 Hz), 128.40, 128.48, 129.12, 136.10, 136.15, 136.41, 136.59, 137.04, 139.44, 139.89, 140.14, 140.22, 141.49, 141.67, 141.88, 142.01, 142.05, 142.09, 142.15, 142.20, 142.26, 142.47, 142.58, 142.60, 142.70, 143.00, 143.18, 144.39, 144.42, 144.63, 144.78, 145.18, 145.28, 145.30, 146.34, 145.42, 145.58, 145.63, 145.78, 145.97, 146.08, 146.14, 146.18, 146.23, 146.30, 146.36, 146.56, 146.81, 147.36, 153.08, 153.14, 153.36, 156.29, 161.10 (dd, $^1J_{FC}$ = 249.7 Hz, $^3J_{FC}$ = 6.3 Hz); UV-vis (CHCl$_3$): λ_{max} (ε) = 256 nm (115 000); MS (FAB) m/z 951 (M$^+$); HRMS calcd for C$_{74}$H$_{11}$F$_2$N 951.0860; found 951.0861; calcd C 93.37, H 1.16, N 1.47; found C 93.47, H 1.67, N 1.45.

C$_{60}$-Fused N-phenyl-2-(2-fluorophenyl)pyrrolidine (3). A toluene solution (100 mL) of the 2-fluorobenzaldehyde (62 mg, 0.5 mmol), N-phenylglycine (151 mg, 1 mmol) and [60]fullerene (360 mg, 0.5 mmol) was stirred at 120 °C for 15 h and concentrated under reduced pressure. The product was separated by column chromatography (SiO$_2$, n-hexane : toluene, 20 : 1–5 : 1) and by GPC to give the compound 3 (72.1 mg, 15.4%); ^{1}H NMR (700 MHz, CDCl$_3$, δ): 5.09 (1H, d, J = 9.9 Hz), 5.65 (1H, d, J = 9.9 Hz), 6.61 (1H, s), 7.02–7.18 (3H, m), 7.20–7.28 (1H, m), 7.28–7.42 (4H, m), 7.84 (1H, dd, J = 6.3, 6.3 Hz); ^{19}F-NMR (372.5 MHz, CDCl$_3$, δ): −114.0 to −115.5 (m); ^{13}C NMR (175 MHz, CDCl$_3$, δ): 67.90 (bs), 68.43, 75.60, 115.93 (d, $^2J_{FC}$ = 22.4 Hz), 120.64 (bs), 122.28 (bs), 124.91, 125.47 (d, $^3J_{FC}$ = 11.7 Hz), 129.38, 129.80 (d, $^3J_{FC}$ = 7.7 Hz), 130.12, 135.44, 135.82, 136.43, 136.57, 139.45, 139.95, 140.26, 140.31, 141.78, 142.04, 142.08, 142.11, 142.15, 142.21, 142.24, 142.32, 142.63, 142.65, 142.67, 142.70, 143.07, 143.13, 144.47, 144.51, 144.56, 144.64, 145.18, 145.27, 145.32, 146.36, 145.52, 145.55, 145.59, 145.60, 145.64, 145.97, 146.04, 146.12, 146.16, 146.19, 146.27, 146.32, 146.36, 146.73, 147.40, 147.44, 152.87, 153.65, 153.91, 156.67, 160.99 (d, $^1J_{FC}$ = 249.9 Hz); UV-vis (CHCl$_3$): λ_{max} (ε) = 256 nm (123 000); MS (FAB) m/z 934 (M + 1); HRMS calcd for C$_{74}$H$_{13}$FN 934.1032; found

934.1023; calcd C 95.17, H 1.30, N 1.50; found C 94.42, H 1.69, N 1.43.

C$_{60}$-Fused N-phenyl-2-(2,6-difluorophenyl)pyrrolidine (4). A toluene solution (100 mL) of the 2,6-difluorobenzaldehyde (36 mg, 0.25 mmol), N-phenylglycine (76 mg, 0.5 mmol) and [60] fullerene (175 mg, 0.25 mmol) was stirred at 120 °C for 48 h and concentrated under reduced pressure. The product was separated by column chromatography (SiO$_2$, n-hexane : toluene, 20 : 1) and by GPC to give the compound 4 (103 mg, 43%); ^{1}H NMR (700 MHz, CDCl$_3$, δ): 5.40 (1H, dd, J = 9.9, 5.9 Hz), 5.66 (1H, dd, J = 9.9, 2.4 Hz), 6.88–7.02 (2H, m), 7.14 (1H, d, J = 7.5 Hz), 7.20–7.30 (3H, m), 7.37 (1H, t, J = 7.5 Hz); ^{19}F-NMR (372.5 MHz, CDCl$_3$, δ): −105.30 to −105.39 (1F, m), −114.35 to −114.45 (1F, m); ^{13}C NMR (175 MHz, CDCl$_3$, δ): 62.81 (dd, $^3J_{FC}$ = 9.2 Hz), 65.26, 68.44, 74.21, 111.67 (d, $^2J_{FC}$ = 24.5 Hz), 112.94 (d, $^2J_{FC}$ = 22.9 Hz), 115.50, 115.64 (t, $^2J_{FC}$ = 34.0 Hz), 119.38, 129.56, 130.59 (t, $^3J_{FC}$ = 10.6 Hz), 134.56, 135.06, 136.26, 137.04, 139.72, 140.16, 140.26, 140.33, 141.71, 141.82, 141.86, 142.10, 142.13, 142.15, 142.22, 142.42, 142.62, 142.65, 142.68, 143.10, 143.18, 144.37, 144.61, 144.66, 145.10, 145.25, 145.29, 146.32, 145.47, 145.57, 145.73, 145.77, 145.97, 146.06, 146.09, 146.11, 146.31, 147.46, 147.55, 151.84, 154.44, 154.78, 155.27, 160.26 (dd, $^1J_{FC}$ = 257.3 Hz, $^3J_{FC}$ = 6.3 Hz), 161.99 (dd, $^1J_{FC}$ = 247.3 Hz, $^3J_{FC}$ = 8.9 Hz); UV-vis (CHCl$_3$): λ_{max} (ε) = 256 nm (119 000); MS (FAB) m/z 951 (M$^+$); HRMS calcd for C$_{74}$H$_{11}$F$_2$N 951.0860; found 951.0867; calcd C 93.37, H 1.16, N 1.47; found C 93.22, H 1.34, N 1.56.

C$_{60}$-Fused N-(2-fluorophenyl)-2-(2-methoxyphenyl) pyrrolidine (5). A chlorobenzene solution (80 mL) of the anisaldehyde (68 mg, 0.5 mmol), N-(2-fluorophenyl)glycine (85 mg, 0.5 mmol) and [60]fullerene (180 mg, 0.25 mmol) was stirred at 130 °C for 96 h and concentrated under reduced pressure. The product was separated by column chromatography (SiO$_2$, n-hexane : toluene, 20 : 1–2 : 1) and by GPC to give the compound 5 (82.5 mg, 34%); ^{1}H NMR (700 MHz, CDCl$_3$, δ): 3.75 (3H, s), 4.71 (1H, d, J = 10.3 Hz), 5.65 (1H, d, J = 10.3 Hz), 6.68 (1H, s), 6.82–6.93 (2H, m), 7.02–7.29 (5H, m), 7.77 (1H, dd, J = 7.9, 1.6 Hz); ^{19}F-NMR (372.5 MHz, CDCl$_3$, δ): −121.23 to −121.34 (m); ^{13}C NMR (175 MHz, CDCl$_3$, δ): 55.29, 66.39, 68.95, 69.16, 74.99, 110.78, 116.28 (d, $^2J_{FC}$ = 20.2 Hz), 121.21, 123.07, 124.42 (d, $^2J_{FC}$ = 11.6 Hz), 125.09, 129.05 (d, $^3J_{FC}$ = 7.6 Hz), 129.72, 134.65, 135.02 (d, $^3J_{FC}$ = 10.2 Hz), 136.63, 136.51, 136.63, 139.33, 140.18, 140.23, 141.50, 141.68, 141.74, 141.82, 142.00, 142.09, 142.17, 142.24, 142.35, 142.55, 142.57, 142.62, 142.65, 142.96, 143.05, 144.36, 144.38, 144.54, 144.61, 145.11, 145.20, 145.27, 145.36, 145.51, 145.55, 145.59, 145.72, 145.90, 145.94, 146.07, 146.15, 146.19, 146.25, 146.54, 146.73, 147.33, 147.38, 153.41, 153.77, 154.71, 156.52, 157.32, 157.58 (d, $^3J_{FC}$ = 245.3 Hz); UV-vis (CHCl$_3$): λ_{max} (ε) = 257 nm (120 000); MS (FAB) m/z 964 (M + 1); HRMS calcd for C$_{75}$H$_{15}$FNO 963.1059; found 963.1036; calcd C 93.45, H 1.46, N 1.45; found C 93.38, H 1.61, N 1.52.

C$_{60}$-Fused N-(2,6-difluorophenyl)-2-(2-methoxyphenyl) pyrrolidine (6). A chlorobenzene solution (200 mL) of the anisaldehyde (136 mg, 1 mmol), N-(2,6-difluorophenyl)glycine (187 mg, 1 mmol) and [60]fullerene (360 mg, 0.5 mmol) was stirred at 140 °C for 96 h and concentrated under reduced pressure. The product was separated by column chromatography (SiO$_2$, n-hexane : toluene, 10 : 1–5 : 1) to give the

compound **6** (219 mg, 45%); ^{1}H NMR (700 MHz, CDCl$_3$, δ): 3.86 (3H, s), 5.20 (1H, d, J = 9.1 Hz), 5.34 (1H, d, J = 9.1 Hz), 6.88–6.95 (2H, m), 6.99–7.07 (2H, m), 7.16 (1H, s), 7.20–7.29 (2H, m), 7.81 (1H, d, J = 7.9 Hz); ^{19}F-NMR (372.5 MHz, CDCl$_3$, δ): −114.80 to −114.98 (m); ^{13}C NMR (175 MHz, CDCl$_3$, δ): 55.41, 65.48, 69.13, 69.95, 111.02, 112.38 (d, $^2J_{FC}$ = 23.9 Hz), 120.82, 122.54, 125.31, 126.26 (t, $^2J_{FC}$ = 21.2 Hz), 128.22, 128.96, 129.32, 134.81, 136.57, 136.66, 139.39, 140.10, 140.17, 141.50, 141.66, 141.75, 141.89, 141.97, 142.07, 142.10, 142.18, 142.28, 142.42, 142.54, 142.63, 142.96, 143.04, 144.32, 144.45, 144.58, 144.63, 145.07, 145.11, 145.12, 145.20, 145.26, 145.28, 145.33, 145.59, 145.60, 145.71, 145.93, 145.96, 146.06, 146.14, 146.20, 146.25, 146.57, 146.85, 147.23, 147.31, 153.21, 153.81, 154.66, 156.78, 157.91, 159.67, 160.81 (dd, $^1J_{FC}$ = 252.4 Hz, $^3J_{FC}$ = 7.7 Hz); UV-vis (CHCl$_3$): λ_{max} (ε) = 257 nm (125 000); MS (FAB) m/z 981 (M$^+$); HRMS calcd for C$_{75}$H$_{13}$F$_2$NO 981.0965; found 981.0972; calcd C 91.74, H 1.33, N 1.43; found C 91.65, H 1.47, N 1.54.

C$_{60}$-Fused N-(2,6-difluorophenyl)-2-(2,6-dimethoxyphenyl) pyrrolidine (7). A chlorobenzene solution (100 mL) of the 2,6-dimethoxybenzaldehyde (166 mg, 1 mmol), N-(2,6-difluorophenyl)glycine (187 mg, 1 mmol) and [60]fullerene (360 mg, 0.5 mmol) was stirred at 140 °C for 48 h and concentrated under reduced pressure. The product was separated by column chromatography (SiO$_2$, n-hexane : toluene, 10 : 1–5 : 1) to give the compound **7** (205 mg, 41%); ^{1}H NMR (700 MHz, CDCl$_3$, δ): 3.66 (3H, s), 3.78 (3H, s), 5.04 (1H, d, J = 9.1 Hz), 5.52 (1H, d, J = 9.1 Hz), 6.38 (1H, d, J = 7.7 Hz), 6.55 (1H, d, J = 7.7 Hz), 6.86–6.95 (1H, m), 6.97–7.06 (1H, m), 7.11–7.20 (2H, m), 7.38 (1H, s); ^{19}F-NMR (372.5 MHz, CDCl$_3$, δ): −119.23 to −118.31 (2F, m); ^{13}C NMR (175 MHz, CDCl$_3$, δ): 54.55, 56.13, 64.96, 69.15, 69.91, 75.73, 104.03, 104.20, 111.81, 111.94 (d, $^4J_{FC}$ = 4.6 Hz), 113.10, 123.34 (t, $^2J_{FC}$ = 20.2 Hz), 124.06 (d–d, $^2J_{FC}$ = 20.2 Hz, 4JFC = 10.2 Hz), 129.71, 134.43, 136.24, 136.88, 137.09, 139.13, 139.70, 139.91, 139.99, 141.36, 141.63, 141.75, 142.06, 142.09, 142.12, 142.39, 142.46, 142.54, 142.56, 143.02, 144.38, 144.59, 144.67, 144.70, 145.05, 145.08, 145.10, 145.13, 145.20, 145.23, 145.24, 145.56, 145.70, 145.73, 145.81, 145.86, 145.90, 145.94, 145.98, 146.12, 146.14, 146.19, 146.24, 146.25, 146.72, 146.96, 147.24, 147.29, 154.34, 154.37, 155.79, 156.85, 159.02, 159.76, 160.17 (dd, $^1J_{FC}$ = 249.9 Hz, $^3J_{FC}$ = 8.8 Hz); UV-vis (CHCl$_3$): λ_{max} (ε) = 257 nm (120 000); MS (FAB) m/z 1012 (M + 1); HRMS calcd for C$_{76}$H$_{16}$F$_2$NO$_2$ 1012.1149; found 1012.1116; calcd C 90.20, H 1.49, N 1.38; found C 90.31, H 1.65, N 1.36.

Acknowledgements

Notes and references

1 L. Dou, J. You, Z. Hong, Z. Xu, G. Li, R. A. Street and Y. Yang, Adv. Mater., 2013, 25, 6642.

2 C.-C. Chueh, C.-Z. Li and A. K.-Y. Jen, Energy Environ. Sci., 2015, 8, 1160.

3 F. C. Krebs, N. Espinosa, M. Hösel, R. R. Søndergaard and M. Jørgensen, Adv. Mater., 2014, 26, 29.

4 R. Po, A. Bernardi, A. Calabrese, C. Carbonera, G. Corso and A. Pellegrino, Energy Environ. Sci., 2014, 7, 925.

5 T. P. Osedach, T. L. Andrewb and V. Bulović, Energy Environ. Sci., 2013, 6, 711.

6 J. Zhao, Y. Li, G. Yang, K. Jiang, H. Lin, H. Ade, W. Ma and H. Yan, Nat. Energy, 2016, 1, 15027.

7 V. Vohra, K. Kawashima, T. Kakara, T. Koganezawa, I. Osaka, K. Takimiya and H. Murata, Nat. Photonics, 2015, 9, 403.

8 L. Huo, T. Liu, X. Sun, Y. Cai, A. J. Heeger and Y. Sun, Adv. Mater., 2015, 27, 2938.

9 J.-D. Chen, C. Cui, Y.-Q. Li, L. Zhou, Q.-D. Ou, C. Li, Y. Li and J.-X. Tang, Adv. Mater., 2015, 27, 1035.

10 Z. He, C. Zhong, S. Su, M. Xu, H. Wu and Y. Cao, Nat. Photonics, 2012, 6, 591.

11 G. Yu, J. Gao, J. C. Hummelen, F. Wudl and A. J. Heeger, Science, 1995, 270, 1789.

12 G. J. Zhao, Y. He and Y. Li, Adv. Mater., 2010, 22, 4355.

13 K. Zhao, Q. Wang, B. Xu, W. Zhao, X. Liu, B. Yang, M. Sun and J. Hou, J. Mater. Chem. A, 2016, 4, 9511.

14 K. Zhao, L. Ye, W. Zhao, S. Zhang, H. Yao, B. Xu, M. Sun and J. Hou, J. Mater. Chem. C, 2015, 3, 9565.

15 Y. He and Y. Li, Phys. Chem. Chem. Phys., 2011, 13, 1970.

16 Y. Yamane, K. Sugawara, N. Nakamura, S. Hayase, T. Nokami and T. Itoh, J. Org. Chem., 2015, 80, 4638.

17 Y. Morinaka, M. Nobori, M. Murata, A. Wakamiya, T. Sagawa, S. Yoshikawa and Y. Murata, Chem. Commun., 2013, 49, 3670.

18 K. Yoshimura, K. Matsumoto, Y. Uetani, S. Sakumichi, S. Hayase, M. Kawatsura and T. Itoh, Tetrahedron, 2012, 68, 3605.

19 P. A. Troshin, E. A. Khakina, M. Egginger, A. E. Goryachev, S. I. Troyanov, A. Fuchsbauer, A. S. Peregudov, R. N. Lyubovskaya, V. F. Razumov and N. S. Sariciftci, ChemSusChem, 2010, 3, 356.

20 K. Matsumoto, K. Hashimoto, M. Kamo, Y. Uetani, S. Hayase, M. Kawatsura and T. Itoh, J. Mater. Chem., 2010, 20, 9226.

21 C. Yang, J. Y. Kim, S. Cho, J. K. Lee, A. J. Heeger and F. Wudl, J. Am. Chem. Soc., 2008, 130, 6444.

22 M. Lenes, G.-J. A. H. Wetzelaer, F. B. Kooistra, S. C. Veenstra, J. C. Hummelen and P. W. M. Blom, Adv. Mater., 2008, 20, 2116.

23 G. Zhao, Y. He, Z. Xu, J. Hou, M. Zhang, J. Min, H.-Y. Chen, M. Ye, Z. Hong, Y. Yang and Y. Li, Adv. Funct. Mater., 2010, 20, 1480.

24 Y. Lin and X. Zhan, Mater. Horiz., 2014, 1, 470.

25 K. Cnops, B. P. Rand, D. Cheyns, B. Verreet, M. A. Empl and P. Heremans, Nat. Commun., 2014, 5, 3406.

26 Y. Liu, T. T. Larsen-Olsen, X. Zhao, B. Andreasen, R. R. Søndergaard, M. Helgesen, K. Norrman, M. Jørgensen, F. C. Krebs and X. Zhan, Sol. Energy Mater. Sol. Cells, 2013, 112, 157.

27 D. Mori, H. Benten, H. Ohkita, S. Ito and K. Miyake, *ACS Appl. Mater. Interfaces*, 2012, **4**, 3325.

28 E. Zhou, J. Cong, M. Zhao, L. Zhang, K. Hashimoto and K. Tajima, *Chem. Commun.*, 2012, **48**, 5283.

29 Y. Vaynzof, T. J. K. Brenner, D. Kabra, H. Sirringhaus and R. H. Friend, *Adv. Funct. Mater.*, 2012, **22**, 2418.

30 M. Schubert, D. Dolfen, J. Frisch, S. Roland, R. Steyrleuthner, B. Stiller, Z. Chen, U. Scherf, N. Koch, A. Facchetti and D. Neher, *Adv. Energy Mater.*, 2012, **2**, 369.

31 A. Facchetti, *Chem. Mater.*, 2011, **23**, 733.

32 M. Karakawa, T. Nagai, K. Adachi, Y. Ie and Y. Aso, *J. Mater. Chem. A*, 2014, **2**, 20889.

33 M. Maggini, G. Scorrano and M. Prato, *J. Am. Chem. Soc.*, 1993, **115**, 9798.

34 P. Wang, B. Chen, R. M. Metzger, T. Da Ros and M. Prato, *J. Mater. Chem.*, 1997, **7**, 2397.

35 J. Pommerehne, H. Vestweber, W. Guss, R. F. Mahrt, H. Bässler, M. Porsch and J. Daub, *Adv. Mater.*, 1995, **7**, 551.

36 G. D. Han, W. R. Collins, T. L. Andrew, V. Bulović and T. M. Swager, *Adv. Funct. Mater.*, 2013, **23**, 3061.

37 M. M. Wienk, J. M. Kroon, W. J. H. Verhees, J. Knol, J. C. Hummelen, P. A. van Hal and R. A. J. Janssen, *Angew. Chem., Int. Ed*, 2003, **42**, 3371.

38 Y. Liang, Z. Xu, J. Xia, S.-T. Tsai, Y. Wu, G. Li, C. Ray and L. Yu, *Adv. Mater.*, 2010, **22**, E135.

39 H. J. Son, W. Wang, T. Xu, Y. Liang, Y. Wu, G. Li and L. Yu, *J. Am. Chem. Soc.*, 2011, **133**, 1885.

40 F. Huang, H. Wu, D. Wang, W. Yang and Y. Cao, *Chem. Mater.*, 2004, **16**, 708.

41 M. A. Khadlm and L. D. Colebrook, *J. Chem. Eng. Data*, 1985, **30**, 239.

42 I. Waterhouse, A. Naylor, C. J. Wallis and F. Ellis, *EP Pat.*, 0340030, 1989.